ARTICLE

Autophagy-dependent removal of α-synuclein: a novel mechanism of GM1 ganglioside neuroprotection against Parkinson's disease

Yu-Lin Guo[1,2], Wen-Jun Duan[1,2], Dan-Hua Lu[1,2], Xiao-Hui Ma[1,2], Xiao-Xiao Li[1,2], Zhao Li[1,2], Wei Bi[3], Hiroshi Kurihara[1,2], Hai-Zhi Liu[3], Yi-Fang Li[1,2] and Rong-Rong He[1,2,4]

GM1 ganglioside is particularly abundant in the mammalian central nervous system and has shown beneficial effects on neurodegenerative diseases. In this study, we investigated the therapeutic effect of GM1 ganglioside in experimental models of Parkinson's disease (PD) in vivo and in vitro. Mice were injected with MPTP (30 mg·kg^{-1}·d^{-1}, i.p.) for 5 days, resulting in a subacute model of PD. PD mice were treated with GM1 ganglioside (25, 50 mg·kg^{-1}·d^{-1}, i.p.) for 2 weeks. We showed that GM1 ganglioside administration substantially improved the MPTP-induced behavioral disturbance and increased the levels of dopamine and its metabolites in the striatal tissues. In the MPP$^+$-treated SH-SY5Y cells and α-synuclein (α-Syn) A53T-overexpressing PC12 (PC12$^{α-Syn\ A53T}$) cells, treatment with GM1 ganglioside (40 μM) significantly decreased α-Syn accumulation and alleviated mitochondrial dysfunction and oxidative stress. We further revealed that treatment with GM1 ganglioside promoted autophagy, evidenced by the autophagosomes that appeared in the substantia nigra of PD mice as well as the changes of autophagy-related proteins (LC3-II and p62) in the MPP$^+$-treated SH-SY5Y cells. Cotreatment with the autophagy inhibitor 3-MA or bafilomycin A1 abrogated the in vivo and in vitro neuroprotective effects of GM1 ganglioside. Using GM1 ganglioside labeled with FITC fluorescent, we observed apparent colocalization of GM1-FITC and α-Syn as well as GM1-FITC and LC3 in PC12$^{α-Syn\ A53T}$ cells. GM1 ganglioside significantly increased the phosphorylation of autophagy regulatory proteins ATG13 and ULK1 in doxycycline-treated PC12$^{α-Syn\ A53T}$ cells and the MPP$^+$-treated SH-SY5Y cells, which was inhibited by 3-MA. Taken together, this study demonstrates that the anti-PD role of GM1 ganglioside resulted from activation of autophagy-dependent α-Syn clearance.

Keywords: Parkinson's disease; GM1 ganglioside; α-synuclein; autophagy; dopamine

INTRODUCTION

Parkinson's disease (PD), one of the most widespread neurodegenerative diseases, affects 2%–3% of the population aged 65 and older [1]. Generally, PD is characterized by selective loss of dopaminergic neurons in the substantia nigra of the midbrain [2]. Researchers have reported multiple molecular mechanisms underlying PD, such as mitochondrial dysfunction, oxidative stress, axonal transport, Ca^{2+} homeostasis, and neuroinflammation [1]. In particular, α-synuclein (α-Syn), the intracellular components of Lewy bodies, is considered to be one of the most important neuropathological hallmarks of PD [3]. The accumulation of α-Syn has been observed in the dopaminergic neurons of PD patients [4], MPTP-treated animals [5], and MPP$^+$-treated neuroblastoma cells [6]. In addition, α-Syn mutations (A30P, A53T, and E46K) have been reported to be the main cause of rare familial PD [3, 7–9]. Accordingly, clearance of α-Syn provides a reasonable therapeutic approach for PD. Autophagy is thought to play a vital role in

degrading intracellular α-Syn aggregates [10–13]. Rapamycin has been shown to decrease α-Syn aggregation by inducing autophagy, thereby protecting against dopaminergic neuron death in vitro and in vivo [14]. Unfortunately, the lack of specificity of rapamycin often results in several side effects, such as oral and respiratory infections, leukopenia, stomatitis, hypercholesterolemia, hypertriglyceridemia, and immunosuppression, and thus limits its application for PD therapy [15]. Hence, there is currently an urgent need to find other candidate PD treatments that can clear α-Syn aggregates but have fewer side effects.

GM1 ganglioside (18:1/18:0) is one of the predominant brain gangliosides, glycosphingolipids composed of three structural units: an oligosaccharide, a ceramide anchor, and several sialic acid residues [16]. This molecule has been viewed as an essential modulator in various brain functions due to its regulation of neuronal plasticity, the release of neurotrophins, neurotransmission, and interactions with neuroregulatory proteins [17, 18]. In

A novel mechanism for GM1 ganglioside against PD
YL Guo et al.

519

addition, exogenous ganglioside has been shown to affect the survival of dopaminergic [19, 20], glutamatergic [21], and cholinergic neurons [22] in the central nervous system. The therapeutic effect of GM1 ganglioside has been shown in PD patients, as well as in MPTP-treated mice and primates [19, 20, 23–26], demonstrating neuroprotective or neurorestorative effects [27–29]. Despite these positive data, the precise mechanism of GM1 ganglioside for treatment of PD is still uncertain. This treatment was suggested to degrade α-Syn in an autophagy-dependent manner in previous reports [30–32], which prompted us to investigate whether autophagy was involved in the anti-PD mechanism of GM1 ganglioside. To prove this hypothesis, we established α-Syn overexpression models by MPTP/MPP$^+$ treatment to evaluate the effects of GM1 both in vivo and in vitro. In addition, we employed PC12$^{α-Syn\ A53T}$ cells expressing inducible α-Syn to demonstrate a direct relationship between GM1 and α-Syn. Our research elucidates a novel mechanism underlying the protective effect of GM1 ganglioside against PD, which provides vital evidence for its clinical usage.

MATERIALS AND METHODS

Reagents and antibodies

MPTP, MPP$^+$, and 3-MA were purchased from Millipore Sigma (St. Louis, MO, USA). GM1 ganglioside was purchased from Qilu Corporation (Ji-nan, China). Selegiline was purchased from Orion Corporation (Turku, Finland). Rapamycin was purchased from Selleck (Houston, TX, USA). Pierce bicinchoninic acid (BCA) protein assay kits were obtained from Thermo Scientific (Rockford, IL, USA). DNA transfection reagent was purchased from Neofect Biotechnology Corporation (Beijing, China). The antibodies used in all experiments were as follows: α-Syn (1:1000, Santa Cruz, Dallas, TX, USA), β-actin (1:3000, Santa Cruz), ULK1 (1:1000, CST, Danvers, MA, USA), p-ULK1^{Ser555} (1:1000, CST), ATG13 (1:1000, CST), ATG13^{Ser355} (1:1000, CST), LC3 (1:1000, CST), SQSTM1/p62 (1:1000, Abcam, Cambridge, UK), and GAPDH (1:3000, Fude Biotechnology, Hangzhou, China). Horseradish peroxidase-conjugated secondary antibodies included HRP AffiniPure Goat Anti-Mouse IgG (H + L) (1:5000, Fude Biotechnology) and HRP AffiniPure Goat Anti-Rabbit IgG (H + L) (1:5000, Fude Biotechnology). The secondary antibodies were conjugated with Alexa Fluor 488 goat antirabbit IgG, Alexa Fluor 555 goat antirabbit IgG or Alexa Fluor 555 goat anti-mouse IgG (1:300, Life Technologies, Grand Island, NY, USA). Nuclear dyes included DAPI (1:800, Beyotime, Shanghai, China) and Hoechst 33258 (Beyotime).

Animals and treatment

The inbred strain of male C57BL/6 J mice at 8–9 weeks old and weighing 20–25 g was purchased from Guangdong Experimental Animal Center in the study. The animals were given free access to food and water. The animal room temperature was 23 ± 2 °C under a 12-h light/12-h dark cycle. All animal experiments were approved by the Animal Ethics Committee of Jinan University (approval number: 20130904001).

Experimental procedures (Supplementary Fig. S1a) were conducted as follows. Eight-week-old male C57BL/6 J mice were randomly divided into 7 groups: control, GM1-H, MPTP, MPTP + GM1-L, MPTP + GM1-H, MPTP + 3-MA + GM1, and MPTP + selegiline (Sele) (n = 15 each group). Except for the control and GM1-high-dose groups, the other groups were injected daily with MPTP (30 mg/kg) intraperitoneally for five days, resulting in a subacute model of PD. Then, the control group and the MPTP group were given an equal volume of saline daily, and the other mice were injected intraperitoneally daily with 25 mg/kg or 50 mg/kg GM1 ganglioside. Then, 15 mg/kg 3-MA and 60 mg/kg selegiline were given daily by intragastric gavage for two consecutive weeks. The intraperitoneal injection of 3-MA was given 30 min before GM1 ganglioside administration.

Rotarod test

Rotarod performance was used to assess the motor balance and coordination of the mice. Motor function was evaluated as described previously [33]. Mice were trained for 3 days prior to treatment to adapt to the rotarod apparatus (Zhenghua Co., Huaibei, China). After training, on the 7th day, the mice were placed in a separate runway on the rod, with a constant speed of 25 rpm every day at the same time. Each mouse was tested at least 3 times. The latency to fall was recorded.

Pole test

The pole test was used to evaluate the mouse movement disorder. The instrument consists of an iron stand (height, 60 cm; diameter, 0.8 cm) with a small ball wrapped with gauze at the top. In the test, the mice were placed on the top of a small ball, and the time required for the mouse to climb down the pole was recorded. The test was performed 3 times per mouse, and the maximum time was recorded.

Gait analysis

Catwalk is a system for rodent gait analysis. The apparatus consists of a long glass walking plate, a fluorescent light beamed into the glass plate and a high-speed video camera under the glass plate. In a dark environment, the light was reflected downward, and a camera mounted under the glass recorded the footprint of the mouse on the walkway [34]. Mice were trained to cross the glass walkway 3 days prior to the test. After the last drug administration, the mice underwent unforced and uninterrupted movement at least 3 times. The mouse gait data were qualitatively and quantitatively analyzed by the automated gait analysis system Catwalk (Noldus Information Technology, Wageningen, the Netherlands).

Dopamine, DOPAC, and HVA measurements

The levels of dopamine and its metabolites (DOPAC and HVA) in the striatum were detected as previously described [35]. In brief, 3 mice from each group were sacrificed, and the striatum was peeled off. The weighed samples were homogenized in 0.3% perchloric acid and then centrifuged at 13,400 × g for 10 min at 4 °C. The supernatants were filtered through a 0.22 μm filter membrane. The mobile phase consisted of 20.2 g of trisodium citrate, 0.036 g of disodium ethylenediamine tetraacetate, 13.64 g of citric acid, 0.18 g of sodium octane sulfonate, 100 mL of methanol and up to 1 L with ultrapure water. The supernatants were used for dopamine, DOPAC, and HVA measurements by HPLC system coupled to an electrochemical detector (ESA Biosciences, Chelmsford, MA, USA) (E1: -150 mV and E3: + 450 mV).

Cell culture

Human neuroblastoma SH-SY5Y cells were kindly provided by Key Lab Innovat Chem Drug Res Cardioceb (Jinan University, Guangzhou, China). PC12$^{α-Syn\ A53T}$ cells were kindly provided by the Chinese Academy of Sciences (Shanghai, China). SH-SY5Y cells were cultured in DMEM supplemented with 10% (v/v) FBS and 100 units/mL penicillin/streptomycin and maintained at 37 °C in humidified 5% CO$_2$. PC12 cell lines express inducible A53T α-Syn, and the cells were cultured in DMEM containing 10% FBS, 5% horse serum, and 100 units/mL penicillin/streptomycin in a 5% CO$_2$ atmosphere. PC12 cells were treated with 1 μg/mL doxycycline in the medium for 12 h to induce cell overexpression of α-Syn. All experiments were performed using cells at a logarithmic phase.

MTT assay

SH-SY5Y cell viability was evaluated by MTT assays in 96-well plates at a density of 4×10^3 cells/well. After treatment, the medium was replaced with DMEM to which MTT (14 μL, 5 mg/mL)

520

reagent was added in each well and incubated with cells at 37 °C for another 4 h. Then, the supernatant was removed, and the cells were lysed in 150 μL of DMSO for 10 min. The absorbance of dissolved formazan was measured in a microplate reader (Sartorius Stedim, Goettingen, Germany) at 570 nm.

Electron microscopic analysis

Fragments from the substantia nigra pars compacta were fixed in 3% glutaraldehyde for 24 h and then postfixed in osmic acid in 1% phosphate buffer for 2 h. Thereafter, the specimens were dehydrated in 50% ethanol for 10 min, 70% ethanol for 10 min, 90% ethanol for 10 min, 90% ethanol: 90% acetone (1:1) for 10 min, 90% acetone for 10 min, and 100% acetone for 10 min and then embedded in EPON capsules. The specimens were cut into ultrathin sections, collected on copper grids, and stained with sodium acetate and lead citrate. Finally, the specimens were imaged by transmission electron microscopy (TEM) (Philips Tecnai 10, Amsterdam, the Netherlands) for ultrastructure analysis.

Mitochondrial membrane potential (MMP, ΔΨm) measurement

SH-SY5Y cells were cultured in six-well plates and treated with the indicated agents. Then, the level of MMP was measured by 5,5′,6,6′-tetrachloro-1,1′,3,3′-tetraethyl-imidacarbocyanine iodide (JC-1) staining. Green fluorescence was detected in the FL1 channel by a flow cytometer equipped with Expo32 ADC (Beckman Coulter, Brea, CA, USA).

Intracellular ROS measurement

The level of intracellular ROS production was measured using a DCFH-DA fluorescence probe. SH-SY5Y cells were cultured in 6-well plates and treated with the indicated drugs. In addition, the cells were incubated with DCFH-DA at 37 °C for 30 min, and DCFH-DA fluorescence intensities were evaluated by fluorescence microscopy with a plate reader at an excitation wavelength of 485 nm and an emission wavelength of 538 nm.

Western blot analysis

The collected cells were homogenized with cell lysis buffer for Western blot and immunoprecipitation (IP) (Beyotime) at 4 °C for 30 min. Cell lysates were centrifuged at $13,400 \times g$ for 15 min at 4 °C, and the supernatant was collected. Then, the protein concentration was measured with a BCA Protein Assay Kit. Equal amounts of protein were separated by 10%–15% SDS-PAGE and transferred to PVDF membranes (Millipore Corporation, Billerica, MA, USA). The membranes were blocked with 5% nonfat milk in Tris-buffered saline with Tween-20 (TBST) at room temperature for 1 h and then incubated with the indicated primary antibody dilutions in TBST overnight at 4 °C. Then, the membranes were washed with TBST and incubated with HRP-conjugated secondary antibodies for 2 h at room temperature. The membranes were visualized using ECL reagent. Immunoreactivity for each protein band intensity was quantified by NIH ImageJ software and normalized to β-actin as a loading control.

Autophagy flux assay

SH-SY5Y cells were transiently transfected with autophagy LC3 double-labeling (mRFP-GFP-LC3) adenovirus (purchased from Hanbio Biotechnology Co., Ltd., Shanghai, China) using Neofect™ DNA transfection reagent according to the manufacturer's protocol. After transfection, the cells were fixed with 4% paraformaldehyde (PFA), and the nuclei were stained with DAPI. Then, the mRFP- and GFP-LC3 puncta in the SH-SY5Y cells were observed using an LSM 700 confocal microscope (Carl Zeiss Corp., Oberkochen, Germany).

Immunofluorescence analysis

Immunofluorescence staining of SH-SY5Y or PC12$^{α-Syn\ A53T}$ cells grown in confocal dishes was conducted. The cultured cells were rinsed with PBS and fixed with 4% PFA for 10 min, permeabilized with 0.2% Triton-X 100 for 10 min, blocked with 3% bovine serum albumin for 45 min, and then incubated with primary antibodies against α-Syn and LC3 followed by secondary antibodies conjugated with Alexa Fluor 555 goat anti-mouse or goat antirabbit IgG or 488 goat antirabbit IgG for 2 h at room temperature. Nuclei were stained with DAPI or Hoechst 33258, and the treated cells were visualized and analyzed using confocal microscopy.

Synthesis steps of GM1-FITC

The chemical process to label GM1 ganglioside with fluorescent FITC was as follows: fluorescent FITC was dissolved in 500 μL of DMSO at a concentration of 10 μg/mL, and then, the FITC solution was mixed with 500 μL of acetic acid, 500 μL of ethanol and 500 μL of ultrapure water to form a reaction system. GM1 ganglioside was added to the above reaction system for 12 h, and the pH of the solution was adjusted to 7.4.

Statistical analysis

All experiments were independently performed at least three times. Data are expressed as the mean ± SEM. Data were statistically analyzed by IBM SPSS Statistics 25.0 (SPSS, Inc., Chicago, IL, USA). Statistical significance was determined using independent-samples t-test and one-way ANOVA with Bonferroni's multiple comparisons test or Dunnett's or LSD post hoc analysis. A value of $P < 0.05$ was defined as statistically significant.

RESULTS

GM1 ganglioside improves MPTP-induced behavioral deficits and rescues the levels of dopamine and its metabolites in C57BL/6 J mice

MPTP is converted to the toxic metabolite MPP$^+$ by the enzyme MAO-B and kills dopaminergic neurons by inhibiting complex I of the mitochondrial electron transport chain [36]. Thus, MPTP and MPP$^+$ are often used to induce a syndrome of neuronal cytotoxicity closely resembling PD in vivo or in vitro, respectively [37, 38]. In this study, C57BL/6 J mice were intraperitoneally injected with MPTP (30 mg/kg) for 5 days to establish a PD model (Supplementary Fig. S1a) to assess the protective effect of GM1 ganglioside (structure shown in Supplementary Fig. S1b). After 2 weeks of treatments, we performed behavioral tests, including the pole test, the rotarod test, and gait analysis by Catwalk. As shown in Fig. 1a, the MPTP-treated mice spent more time climbing the pole than the control mice ($P < 0.01$). In contrast, the administration of GM1 ganglioside (i.p., 25 and 50 mg/kg) and selegiline (an MAO-B inhibitor, i.g., 60 mg/kg) significantly reduced the time the MPTP-treated mice spent climbing the pole. In the rotarod test, MPTP treatment significantly reduced the latency to fall (Fig. 1b, $P < 0.05$), illustrating the motor deficits induced by MPTP. Treatment with GM1 ganglioside (i.p., 25 and 50 mg/kg) and selegiline inhibited the decline in latency to fall induced by MPTP (Fig. 1b).

Gait disturbances are one of the most common locomotor dysfunctions. We further evaluated the therapeutic effect of GM1 ganglioside on the gait by Catwalk assays with parameters including step cycle, swing speed, cadence, run duration and walking speed. As shown in Fig. 1c–g, a significant decrease was observed in the swing speed and cadence, while a substantial increase was observed in the step cycle, run duration, and walking speed in the MPTP-treated mice. By comparison, treatment with GM1 ganglioside and selegiline effectively ameliorated the impairment of these gait behaviors caused by MPTP (Fig. 1c–g). Moreover, GM1 ganglioside treatment recovered the gait performance (Fig. 1k), increased the touch and suspension times of the limbs (Fig. 1l) and augmented the number of footfall patterns (Fig. 1m) in the MPTP-treated mice. These three behavioral tests
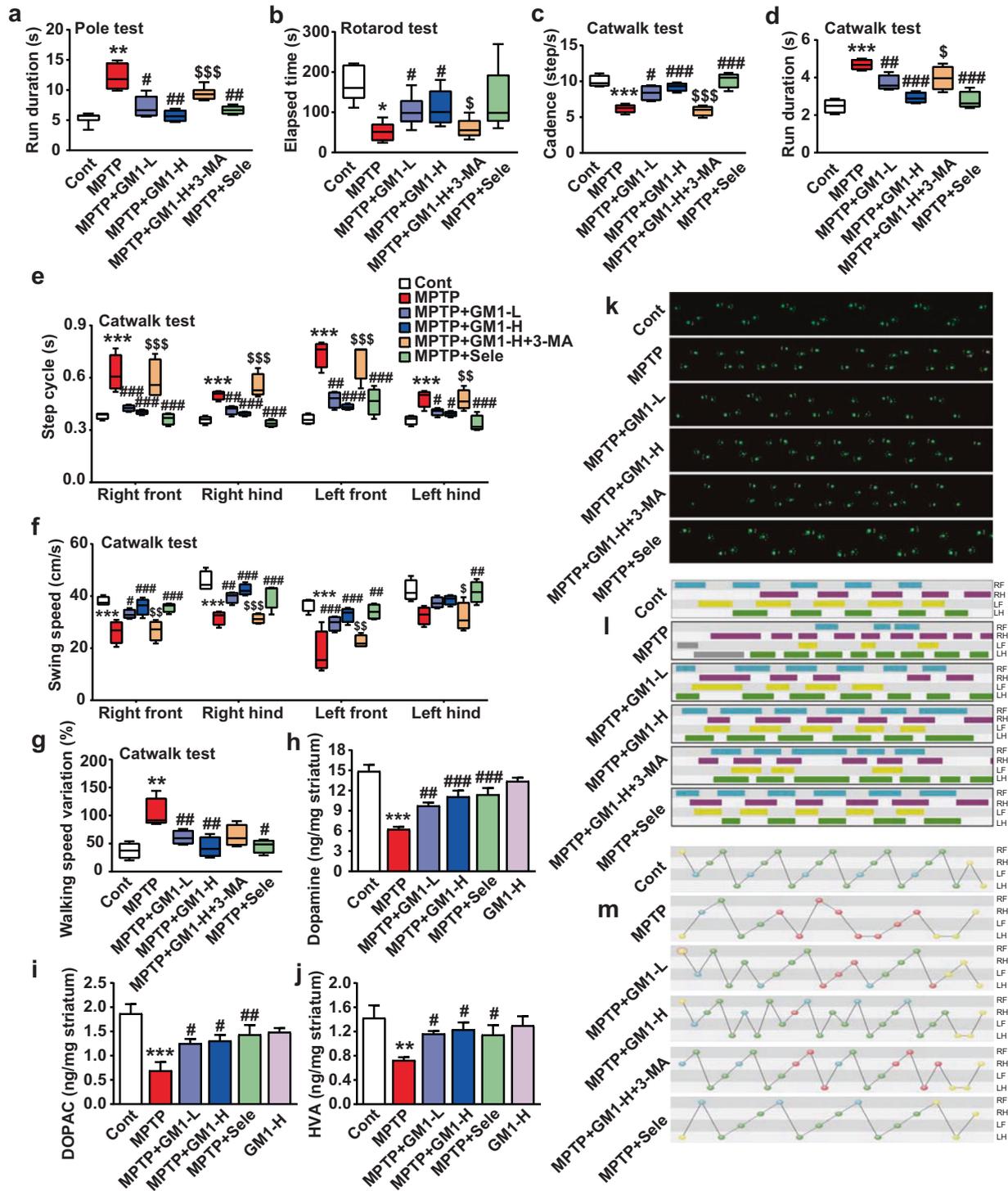
A novel mechanism for GM1 ganglioside against PD
YL Guo et al.

521

Fig. 1 GM1 ganglioside treatment improves the progression of disease in MPTP-treated mice. a, b The run duration on the climbing-pole test and the elapsed time in the rotarod test of mice ($n \geq 6$ mice each group). **e, f** The step cycle and swing speed of all limbs of mice in the Catwalk assay ($n = 4$ mice per group). **c, d,** and **g** The cadence, run duration, and walking speed variation of mice in the Catwalk assay ($n = 4$ mice in each group). **h, i,** and **j** Levels of dopamine, DOPAC, and HVA in the striatum of the MPTP-treated mice were measured by HPLC-ECD ($n = 3$ mice per group). **k, l,** and **m** Representative illuminations in footprint view, timing view and footfall patterns of the mice. Data are expressed as the mean ± SEM. For **a**, the data were analyzed using one-way ANOVA with Dunnett's T3 post hoc test. For **b** and **e**, the data were analyzed using independent-samples t-tests. For **c** and **g**, the data were analyzed using one-way ANOVA with Bonferroni's multiple comparisons test. For **d, f,** and **h–j**, the data were analyzed using one-way ANOVA with LSD post hoc test. Significance is shown as $^*P < 0.05$, $^{**}P < 0.01$, $^{***}P < 0.001$ vs. the control group; $^\#P < 0.05$, $^{\#\#}P < 0.01$, $^{\#\#\#}P < 0.001$ vs. the MPTP group; $^\$P < 0.05$, $^{\$\$}P < 0.01$, $^{\$\$\$}P < 0.001$ vs. the MPTP + GM1-H group.

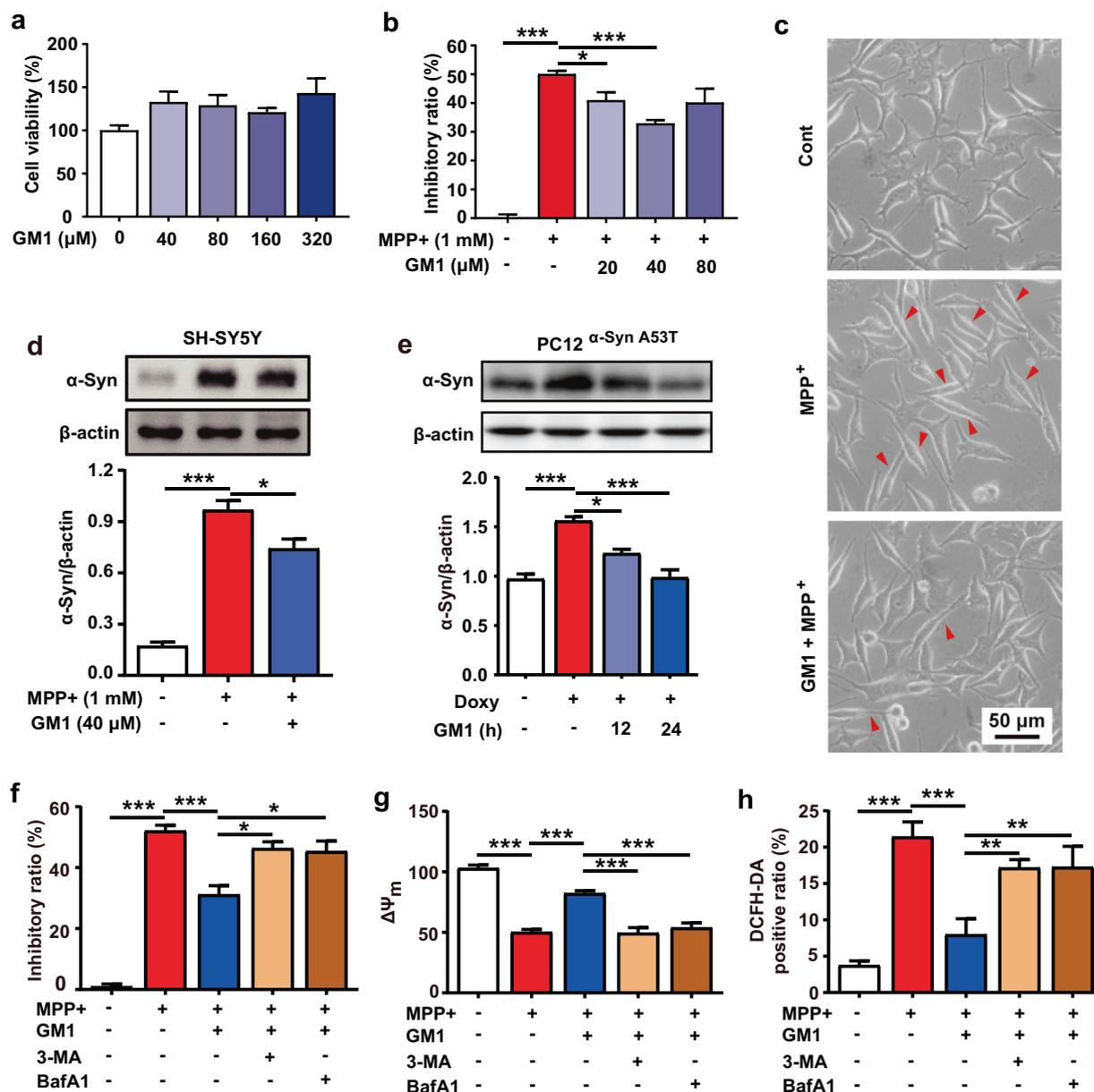A novel mechanism for GM1 ganglioside against PD
YL Guo et al.

522

Fig. 2 GM1 ganglioside has therapeutic potential in the MPP+-treated SH-SY5Y cells. a SH-SY5Y cells were treated with 40, 80, 160 or 320 μM GM1 ganglioside for 24 h. Then, the cell viability was determined by MTT assays ($n = 5$). **b** MPP+ (1 mM) was added to SH-SY5Y cells for 36 h and then replaced with 20, 40 or 80 μM GM1 ganglioside for 24 h. The inhibitory ratio was determined by MTT assays ($n = 3$). **c** Morphological images of SH-SY5Y cells treated with MPP+ for 36 h and then with or without GM1 ganglioside (40 μM) for 24 h. The red arrow represents damaged cells. Scale bar: 50 μm. **d** SH-SY5Y cells were treated with or without MPP+ for 36 h and then replaced with or without GM1 ganglioside for 24 h. The level of α-Syn was analyzed by Western blots. Quantitative analysis of α-Syn relative to β-actin ($n = 3$). **e** Representative Western blot and quantification of α-Syn. PC12$^{\alpha\text{-Syn A53T}}$ cells were treated with or without doxycycline (Doxy) for 12 h and then GM1 ganglioside for 12 h or 24 h ($n = 3$). **f, g**, and **h** MPP+ was added to SH-SY5Y cells for 36 h with GM1 ganglioside, with or without 5 mM 3-MA and with or without 100 nM bafilomycin A1 (BafA1). Then, the cell viability was determined by an MTT assay, and the mitochondrial membrane potential ($\Delta\Psi_m$) and the percentage of DCFH-DA-positive SH-SY5Y cells were determined by flow cytometry ($n = 3$). Data are expressed as the mean ± SEM. For **a, b**, an independent-samples t-test was used for statistical analysis. For **d–g**, one-way ANOVA with Bonferroni's multiple comparisons test was used for statistical analysis. For **h**, one-way ANOVA with LSD post hoc test was used for statistical analysis. $^*P < 0.05$, $^{**}P < 0.01$, $^{***}P < 0.001$.

together suggested a notable therapeutic effect of GM1 ganglioside on PD. Notably, the protective effect of GM1 ganglioside in the three behavior tests was drastically reversed by the administration of 3-MA (i.p., 15 mg/kg), a class III PI3K autophagy inhibitor (Fig. 1a–g and k–m). This finding indicated that autophagy might be associated with the protective effect of GM1 ganglioside.

In addition, we detected the levels of dopamine and its metabolites in the striatum of the mice by high-performance liquid chromatography with electrochemical detection (HPLC-ECD). As shown in Fig. 1h–j, MPTP treatment significantly reduced the levels of dopamine, dihydroxyphenylacetic acid (DOPAC), and homovanillic acid (HVA). Treatment with GM1 ganglioside and selegiline prevented the MPTP-induced reductions of dopamine,
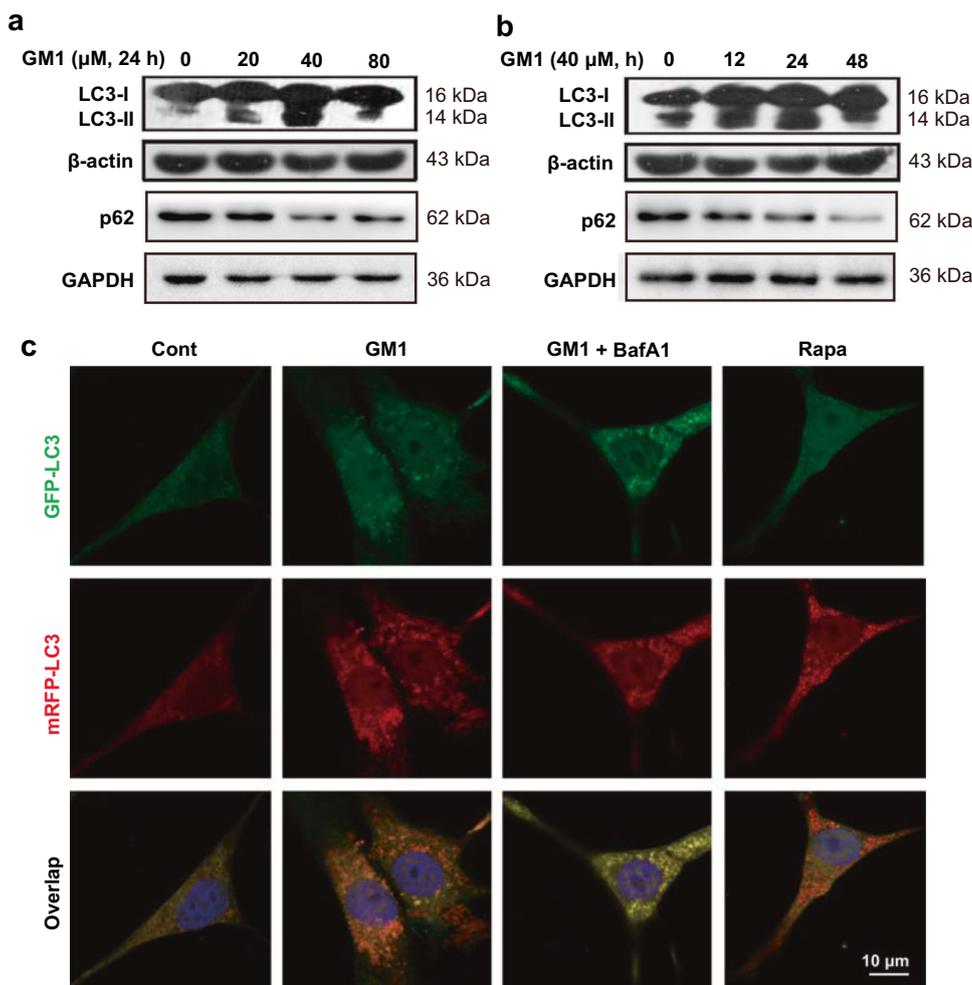
A novel mechanism for GM1 ganglioside against PD
YL Guo et al.

523

Fig. 3 GM1 ganglioside activates autophagy in SH-SY5Y cells. a SH-SY5Y cells were treated with 20, 40, or 80 µM GM1 ganglioside for 24 h. **b** SH-SY5Y cells were treated with 40 µM GM1 ganglioside for 12, 24, or 48 h. The protein levels of LC3 and p62 were analyzed by Western blot analysis. **c** SH-SY5Y cells were transfected with adenovirus expressing mRFP-GFP-LC3, followed by treatment with GM1 ganglioside (40 µM), bafilomycin A1 (BafA1, 100 nM) or rapamycin (50 µM) for 24 h. The LC3 puncta were observed by confocal microscopy. Red (mRFP$^+$/GFP$^-$) puncta indicate autolysosomes, while yellow (mRFP$^+$/GFP$^+$) puncta indicate autophagosomes. Scale bar: 10 µm.

DOPAC, and HVA levels, suggesting that GM1 ganglioside effectively improved the function of dopaminergic neurons.

GM1 ganglioside ameliorates MPP$^+$-induced neurotoxicity and reduces α-Syn accumulation in neuronal cells
MPP$^+$, the metabolite of MPTP, can lead to neurotoxicity in vitro [39, 40]. Thus, we further employed MPP$^+$ to confirm the neuroprotective effect of GM1 ganglioside in SH-SY5Y cells. As shown in Fig. 2a, GM1 ganglioside at concentrations less than 320 µM did not trigger any cytotoxicity. MPP$^+$ (1 mM) substantially inhibited cell proliferation, which was significantly attenuated by treatment with different concentrations (20, 40, and 80 µM) of GM1 ganglioside (Fig. 2b). Moreover, MPP$^+$ led to obvious morphological changes in cells, such as decreased pseudopodia and elongated cell bodies, which were attenuated by GM1 ganglioside (Fig. 2c). Western blot analysis showed that treatment with GM1 ganglioside dramatically inhibited the MPP$^+$-induced α-Syn accumulation in SH-SY5Y cells (Fig. 2d, $P < 0.05$). Consistently, GM1 ganglioside reduced the doxycycline-induced α-Syn over-expression in a time-dependent manner in PC12$^{\alpha-Syn\ A53T}$ cells (Fig. 2e).

Defective mitochondrial function and increased oxidative stress have been demonstrated in the pathogenesis of PD [41]. As shown in Fig. 2g and h, exposure of SH-SY5Y cells to 1 mM MPP$^+$ for 36 h obviously reduced the mitochondrial membrane potential (ΔΨ$_m$) while increasing the ROS levels in SH-SY5Y cells ($P < 0.001$), whereas treatment with GM1 ganglioside markedly inhibited these changes.

In addition, the autophagy inhibitor 3-MA or bafilomycin A1 could abrogate the effect of GM1 ganglioside on the MPP$^+$-induced inhibition of cell viability (Fig. 2f, $P < 0.05$), decrease in ΔΨ$_m$ (Fig. 2g, $P < 0.001$) and ROS generation (Fig. 2h, $P < 0.01$). Consistent with the observation in MPTP-treated mice, these in vitro findings further implied that autophagy activation was involved in the protective effect of GM1 ganglioside on PD.

GM1 ganglioside induces autophagy in neuronal cells
GM1 ganglioside was shown to exhibit a positive effect on inducing autophagy in multiple cell lines [42–44]. Our data showed that the increase in the autophagy marker LC3-II and the degradation of the autophagy substrate SQSTM1/p62 were both enhanced in the SH-SY5Y cells treated with different doses of GM1 ganglioside, especially at 40 µM (Fig. 3a). In addition, at this dose, GM1 ganglioside showed the most obvious effect on these autophagy-related proteins when the cells were treated for 24 h (Fig. 3b). Therefore, in the following experiments, we applied 40 µM and 24 h of GM1 ganglioside as the cell-treatment conditions. To evaluate the GM1-mediated promotion of
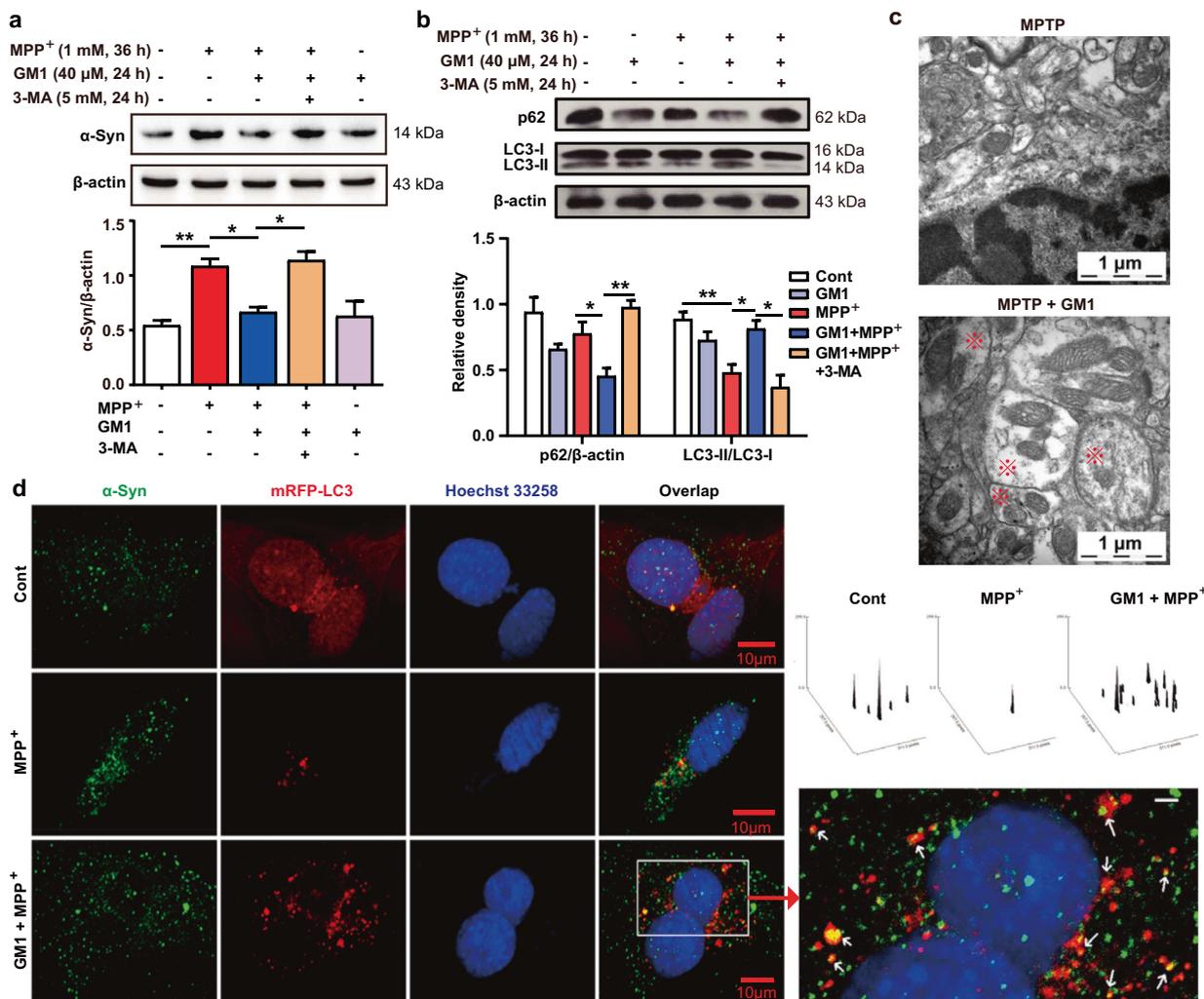
A novel mechanism for GM1 ganglioside against PD
YL Guo et al.

524

Fig. 4   GM1 ganglioside enhances α-Syn clearance and promotes autophagy in MPP+-treated SH-SY5Y cells. a SH-SY5Y cells were treated with the indicated drugs. The protein level of α-Syn was analyzed by Western blots. Quantitative analysis of α-Syn relative to β-actin ($n = 3$, one-way ANOVA followed by Bonferroni's multiple comparisons test). **b** SH-SY5Y cells were treated with the indicated drugs. The protein levels of p62 and LC3 were analyzed by Western blots. Quantitative analysis of p62 relative to β-actin and the ratio of LC3-II/LC3-I ($n = 3$, the data were analyzed using independent-samples t test). Data are expressed as the mean ± SEM. *$P < 0.05$, **$P < 0.01$. **c** Representative pictures of the substantia nigra of the mice treated with or without GM1 ganglioside and MPTP analyzed by transmission electron microscopy. Red "※" represents autophagosomes. Scale bar: 1 μm. **d** The left picture: representative illuminations of mRFP-LC3 and α-Syn signals under confocal microscopy. SH-SY5Y cells were transfected with plasmids expressing mRFP-LC3. Thirty-six hours after transfection, the cells were treated with MPP+ for 36 h and then treated with GM1 ganglioside for another 24 h. The top right picture: three-dimensional graphs of the colocalized puncta of mRFP-LC3 and α-Syn signals. The ordinate represents the fluorescence intensity, and the X and Y axes represent the relative spatial position of the colocalized site. The bottom right picture: a higher magnification of the left picture showing the colocalization of LC3 and α-Syn particles; the right arrow indicates the autolysosome (scale bar, left side: 10 μm and right side: 2 μm).

autophagy more intuitively, we conducted an autophagy flux assay by using mRFP-GFP-LC3 labeling. SH-SY5Y cells were treated with GM1 ganglioside with or without bafilomycin A1. Rapamycin, functioning as an autophagy inducer by inhibiting mTOR [45], was applied as a positive control. Since GFP is sensitive to low pH conditions, when autophagosomes fuse with lysosomes, GFP (green) fluorescence is quenched, and only mRFP (red) fluorescence can be observed. When GFP and mRFP (yellow) fluorescence appear at the same time, it suggests that autophagosomes do not combine with lysosomes [46]. The red puncta were significantly increased in the cells treated with GM1 ganglioside or rapamycin compared with the control cells, while treatment with a combination of GM1 ganglioside and bafilomycin A1 could enhance the yellow puncta (Fig. 3c), indicating that GM1 ganglioside enhanced autophagy flux in SH-SY5Y cells.

The activation of autophagy facilitates the clearance of α-Syn by GM1 ganglioside

Since the removal of aberrant α-Syn offers a promising strategy for the treatment of PD [47], earlier studies have shown that autophagy-mediated α-Syn degradation favors the protective effect against PD [30–32]. The protective effects of GM1 ganglioside on the MPTP-induced mice and the MPP+-induced cells were blocked by 3-MA and bafilomycin A1, indicating that autophagy activation might be involved. As expected, 3-MA substantially abrogated the effect of GM1 ganglioside on decreasing α-Syn protein levels in the MPP+-treated SH-SY5Y cells (Fig. 4a, $P < 0.05$).

We further determined the influence of GM1 ganglioside on the autophagic process. Our data showed that the conversion of LC3-I to LC3-II in SH-SY5Y cells was obviously promoted by GM1 ganglioside treatment in the presence of MPP+ (Fig. 4b). The expression of the autophagy substrate SQSTM1/p62 was also
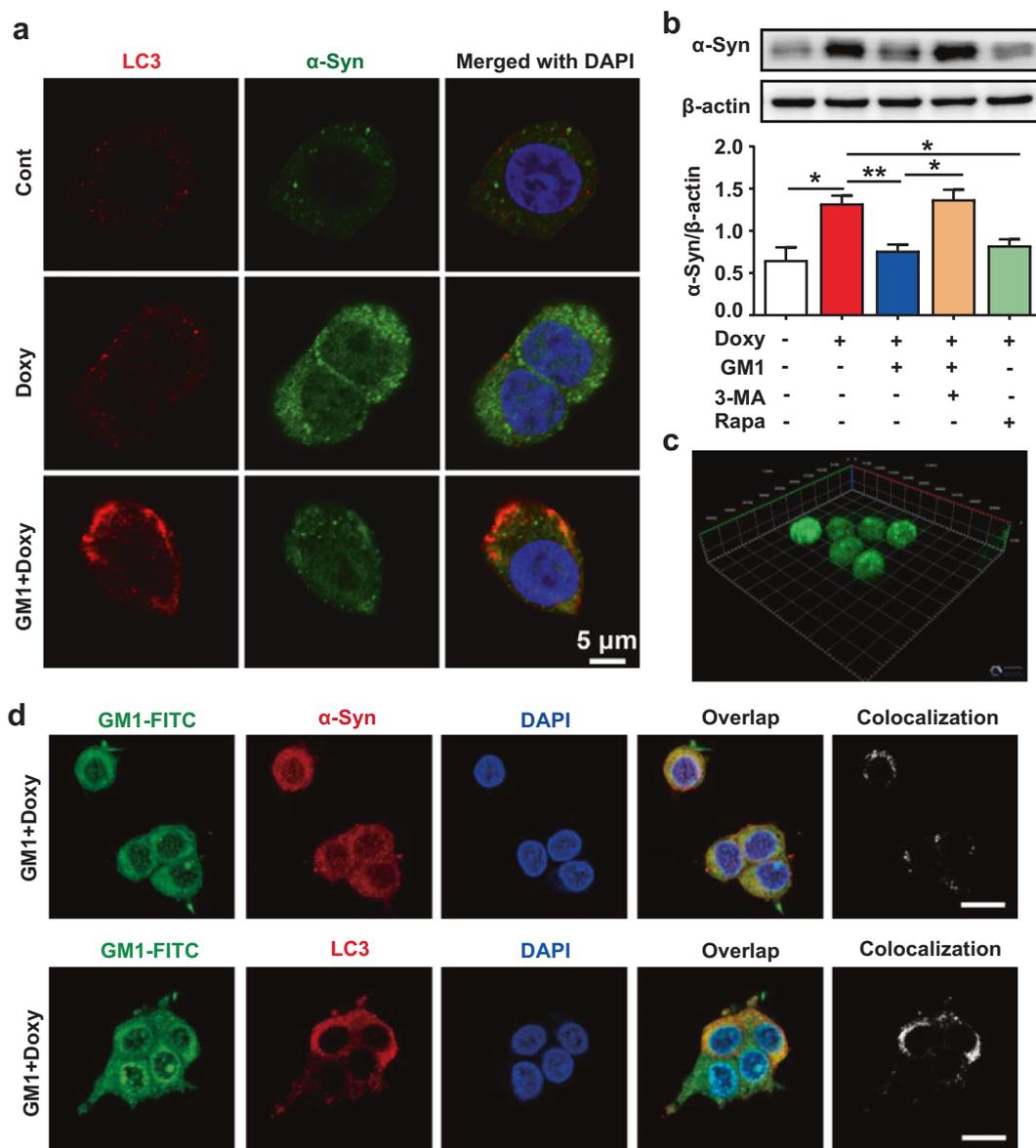
A novel mechanism for GM1 ganglioside against PD
YL Guo et al.

525

Fig. 5 GM1 ganglioside increases α-Syn clearance through autophagy and induces the colocalization of α-Syn and LC3 in PC12$^{α-Syn\ A53T}$ cells. a Expression of α-Syn and LC3 in PC12$^{α-Syn\ A53T}$ cells treated with or without GM1 ganglioside for 24 h was visualized using immunofluorescence. Representative images show that GM1 ganglioside induced the colocalization of LC3 and α-Syn. Scale bar: 5 μm. **b** PC12$^{α-Syn\ A53T}$ cells were treated with or without doxycycline for 12 h and treated with GM1 ganglioside, 3-MA, or rapamycin for 24 h. The α-Syn protein was examined by Western blots. Quantitative analysis of α-Syn to β-actin ($n = 3$). Data are expressed as the mean ± SEM. The data were analyzed using independent samples t tests. The difference was considered significant at $^*P < 0.05$, $^{**}P < 0.01$. **c** Three-dimensional distribution of GM1-FITC in PC12$^{α-Syn\ A53T}$ cells. Representative images show that GM1 ganglioside can enter and evenly distribute in cells. **d** PC12$^{α-Syn\ A53T}$ cells were treated with doxycycline for 12 h, followed by treatment with GM1 ganglioside for 24 h. GM1-FITC, α-Syn, and LC3 were observed using a confocal fluorescence microscope. Scale bar: 10 μm.

reduced by GM1 ganglioside in the MPP$^+$-treated cells (Fig. 4b). Moreover, TEM revealed obvious autophagic vesicles in the substantia nigra of the GM1 ganglioside-treated mice (Fig. 4c). Importantly, confocal microscopy images revealed that GM1 ganglioside-induced autophagosomes were colocalized with α-Syn induced by MPP$^+$ treatment (Fig. 4d). These in vivo and in vitro data indicated that GM1 ganglioside activated autophagy, which participated in α-Syn clearance.

Furthermore, we used PC12$^{α-Syn\ A53T}$ cells, in which the expression of α-Syn A53T can be induced by doxycycline treatment, to confirm the effect of GM1 ganglioside on autophagy and α-Syn removal. The results of confocal microscopy (Fig. 5a) showed that LC3 puncta were increased while

doxycycline-induced α-Syn accumulation was reduced by GM1 ganglioside treatment in PC12$^{α-Syn\ A53T}$ cells, in which the colocalization of LC3 and α-Syn was substantially enhanced (Fig. 5a). Western blot analysis confirmed that GM1 ganglioside caused a decline in the α-Syn protein level, which was reversed by 3-MA cotreatment (Fig. 5b). Similar to GM1 ganglioside, the classic autophagy inducer rapamycin could also strongly decrease the α-Syn levels (Fig. 5b).

We employed a chemical reaction approach to label GM1 ganglioside with fluorescent FITC fluorescent. Strong green fluorescence was observed in PC12$^{α-Syn\ A53T}$ cells treated with GM1-FITC (Fig. 5c). Apparent colocalization was observed in the PC12$^{α-Syn\ A53T}$ cells between GM1-FITC and α-Syn, as well as
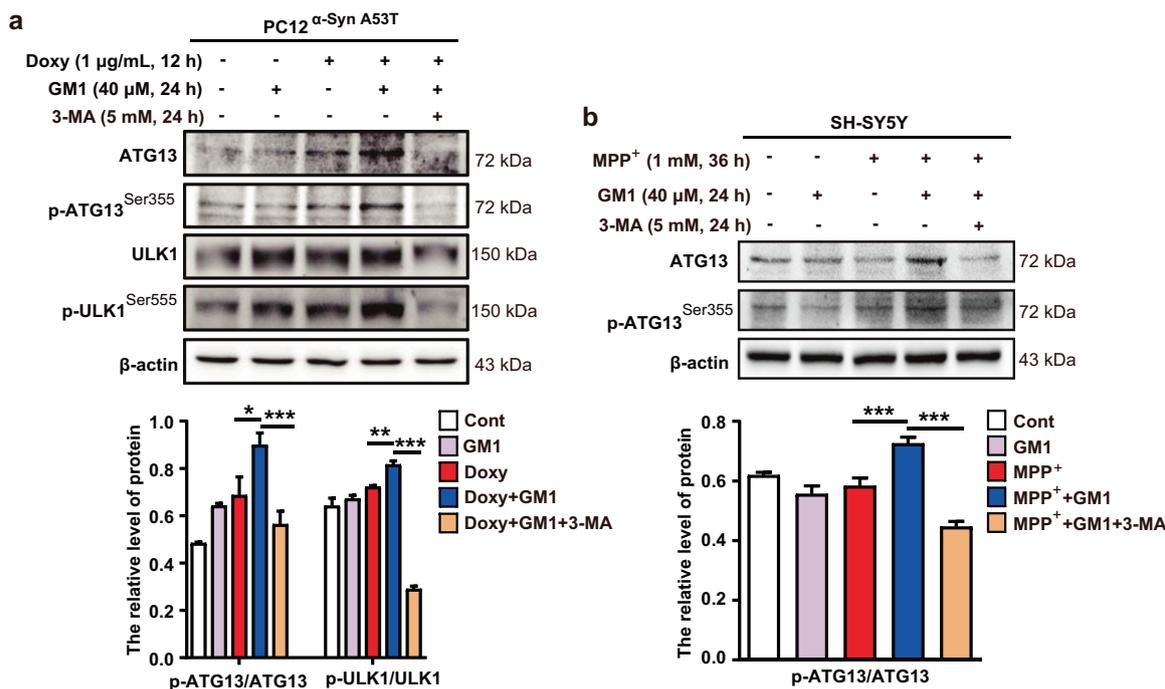
A novel mechanism for GM1 ganglioside against PD
YL Guo et al.

526

Fig. 6 Effect of GM1 ganglioside on the phosphorylation of ATG13 and ULK1. a PC12$^{α\text{-Syn A53T}}$ cells were treated with or without doxycycline for 12 h, followed by treatment with GM1 ganglioside for 24 h and with or without 3-MA. The expression levels of ATG13, p-ATG13^{ser355}, ULK1, and p-ULK1^{ser555} were examined by Western blots. The quantification of the ratio of p-ATG13^{ser355}/ATG13 and p-ULK1^{ser555}/ULK1 ($n = 3$). **b** Western blot analysis to confirm the protein levels of ATG13 and pATG13^{ser355} in SH-SY5Y cells. MPP$^+$ was added to SH-SY5Y cells for 36 h and then replaced with GM1 ganglioside with or without 3-MA for 24 h. Quantification of the ratio of p-ATG13^{ser355}/ATG13 ($n = 3$). Data are represented as the mean ± SEM. One-way ANOVA with LSD post hoc test was used for statistical analysis. $^*P < 0.05$, $^{**}P < 0.01$, $^{***}P < 0.001$.

GM1-FITC and LC3 (Fig. 5d). Taken together, these data indicate that GM1 ganglioside activates autophagy to remove the aggregation of α-Syn.

The ATG13-ULK1 complex is involved in GM1 ganglioside-induced autophagy
The ULK complex consists of ULK1, ATG13, FIP200, and ATG101, which are required to initiate the autophagic process [48, 49]. We evaluated the effects of GM1 ganglioside on the protein expression levels of ULK1 and ATG13. Notably, GM1 ganglioside treatment promoted the phosphorylation of ATG13 and ULK1 in doxycycline-treated PC12$^{α\text{-Syn A53T}}$ cells (Fig. 6a). Nevertheless, the effect of GM1 ganglioside was suppressed by 3-MA treatment (Fig. 6a). Similarly, the GM1 ganglioside-treated SH-SY5Y cells also showed an increased ratio of p-ATG13/ATG13, and 3-MA treatment inhibited this effect of GM1 ganglioside (Fig. 6b). Taken together, the results revealed that GM1 ganglioside induced autophagy by activating the ATG13-ULK1 complex.

DISCUSSION
It has been reported that GM1 ganglioside could modify α-Syn toxicity in the α-Syn model of PD [50]. However, the mechanism by which GM1 ganglioside reduces α-Syn accumulation remains unclear. In the present study, GM1 ganglioside showed an obvious protective effect against PD in the in vivo and in vitro MPTP/MPP$^+$ models. Our results further clearly indicated that GM1 ganglioside directly reduced the accumulation of α-Syn by using doxycycline-treated PC12$^{α\text{-Syn A53T}}$ cells.

Currently, levodopa, monoamine oxidase type B inhibitors or dopamine agonists are frequently used for PD treatment, but they exhibit fluctuations in motor control and abnormal involuntary movements after high-dose treatment or long-term usage [51–53]. In addition, 5-HT$_{1A}$ receptor agonists [54, 55] and cholinergic

inhibitors [56] have also been proven to have therapeutic effects on PD, but these drugs present side effects associated with cognition [57]. Hence, treatments with fewer side effects are urgently required. Interestingly, some autophagic agents offer new perspectives in the treatment of PD. For example, trehalose (an autophagy enhancer) [58, 59], isorhynchophylline (a natural alkaloid) [60], latrepirdine (a neuroactive compound) [61] and nilotinib (a tyrosine kinase inhibitor) [62] were shown to promote autophagy to degrade mutant α-Syn in a PD model. Therefore, autophagy activators show promise in the treatment of PD.

Previous reports have shown that the ganglioside mix containing GM1 can induce autophagy and induce the accumulation of autophagosomes in astrocytes [43, 44] and in β-gal-deficient mouse brains [63]. GM1 was also demonstrated to decrease the toxicity induced by Aβ$_{(1-42)}$ by increasing the expression of autophagic markers and enhancing autophagy in vivo or in vitro [42]. In this study, our results indicated that the cytoprotection of GM1 ganglioside against the accumulation of α-Syn was associated with the enhancement of autophagy, indicated by the increased conversion of LC3-I to LC3-II, the decreased SQSTM1/p62 expression, and the enhanced colocalization of α-Syn and LC3. The ULK complex formed by ULK1, ATG13, ATG101, and FIP200 is required to promote the autophagic process [64]. Moreover, ULK1 could increase the phosphorylation of ATG13 and interact with ATG101 and FIP200 to form the ULK complex, which eventually triggers autophagy [65, 66]. ATG13 and FIP200 are critical for the correct localization of ULK1 to pre-autophagosomes and the stability of the ULK1 protein, and the ULK complex is a node that integrates incoming autophagic signals into autophagosome biogenesis [48]. Our data found that GM1 ganglioside could induce cytoprotective autophagy by upregulating the ATG13-ULK1 complex in different neuronal cells, including human neuroblastoma SH-SY5Y cells and PC12-inducible α-Syn A53T cells. Although ATG13-ULK1 was preliminarily identified as a target, the

A novel mechanism for GM1 ganglioside against PD
YL Guo et al.

527

interaction between GM1 ganglioside and ATG13-ULK1 requires further investigation.

In summary, our findings demonstrate that the activation of autophagy accounts for the anti-PD effect of GM1 ganglioside and provides a potential theoretical basis for the mechanism of GM1 ganglioside in the clearance of α-Syn.

AUTHOR CONTRIBUTIONS
YLG and WJD contributed equally to this work. WJD and RRH designed the project. YLG, DHL, XHM, XXL, and ZL carried out all the experiments. YLG, WJD, DHL, XXL, ZL, WB, and HZL contributed to the statistical analyses and interpretation of the results. YLG and WJD contributed to drafting of the manuscript. WJD, HK, YFL, and RRH revised the paper. All authors edited and agreed to the final version of the manuscript.

ADDITIONAL INFORMATION
The online version of this article (https://doi.org/10.1038/s41401-020-0454-y) contains supplementary material, which is available to authorized users.

Competing interests: The authors declare no competing interests.

REFERENCES
1. Poewe W, Seppi K, Tanner CM, Halliday GM, Brundin P, Volkmann J, et al. Parkinson disease. Nat Rev Dis Prim. 2017;3:21.
2. de Lau LML, Breteler MMB. Epidemiology of Parkinson's disease. Lancet Neurol. 2006;5:525–35.
3. Spillantini MG, Schmidt ML, Lee VM, Trojanowski JQ, Jakes R, Goedert M. Alpha-synuclein in Lewy bodies. Nature. 1997;388:839–40.
4. Holmqvist S, Chutna O, Bousset L, Aldrin-Kirk P, Li W, Bjorklund T, et al. Direct evidence of Parkinson pathology spread from the gastrointestinal tract to the brain in rats. Acta Neuropathol. 2014;128:805–20.
5. Vila M, Vukosavic S, Jackson-Lewis V, Neystat M, Jakowec M, Przedborski S. Alpha-synuclein up-regulation in substantia nigra dopaminergic neurons following administration of the Parkinsonian toxin MPTP. J Neurochem. 2000;74:721–9.
6. Kalivendi SV, Cunningham S, Kotamraju S, Joseph J, Hillard CJ, Kalyanaraman B. Alpha-synuclein up-regulation and aggregation during MPP+-induced apoptosis in neuroblastoma cells: intermediacy of transferrin receptor iron and hydrogen peroxide. J Biol Chem. 2004;279:15240–7.
7. Polymeropoulos MH, Lavedan C, Leroy E, Ide SE, Dehejia A, Dutra A, et al. Mutation in the alpha-synuclein gene identified in families with Parkinson's disease. Science. 1997;276:2045–7.
8. Krüger R, Kuhn W, Müller T, Woitalla D, Graeber M, Kösel S, et al. Ala30Pro mutation in the gene encoding alpha-synuclein in Parkinson's disease. Nat Genet. 1998;18:106–8.
9. Zarranz JJ, Alegre J, Gómez-Esteban JC, Lezcano E, Ros R, Ampuero I, et al. The new mutation, E46K, of alpha-synuclein causes Parkinson and Lewy body dementia. Ann Neurol. 2004;55:164–73.
10. Brundin P, Dave KD, Kordower JH. Therapeutic approaches to target alpha-synuclein pathology. Exp Neurol. 2017;298:225–35.
11. Decressac M, Mattsson B, Weikop P, Lundblad M, Jakobsson J, Björklund A. TFEB-mediated autophagy rescues midbrain dopamine neurons from α-synuclein toxicity. Proc Natl Acad Sci USA. 2013;110:E1817–E1826.
12. Decressac M, Björklund A. TFEB: pathogenic role and therapeutic target in Parkinson disease. Autophagy. 2013;9:1244–6.
13. Spencer B, Potkar R, Trejo M, Rockenstein E, Patrick C, Gindi R, et al. Beclin 1 gene transfer activates autophagy and ameliorates the neurodegenerative pathology in alpha-synuclein models of Parkinson's and Lewy body diseases. J Neurosci. 2009;29:13578–88.
14. Malagelada C, Jin ZH, Jackson-Lewis V, Przedborski S, Greene LA. Rapamycin protects against neuron death in in vitro and in vivo models of Parkinson's disease. J Neurosci. 2010;30:1166–75.
15. Bové J, Martínez-Vicente M, Vila M. Fighting neurodegeneration with rapamycin: mechanistic insights. Nat Rev Neurosci. 2011;12:437–52.
16. Macher BA, Sweeley CC. Glycosphingolipids: structure, biological source, and properties. Methods Enzymol. 1978;50:236–51.
17. Lim ST, Esfahani K, Avdoshina V, Mocchetti I. Exogenous gangliosides increase the release of brain-derived neurotrophic factor. Neuropharmacology. 2011;60:1160–7.
18. Furukawa K, Ohmi Y, Ohkawa Y, Tokuda N, Kondo Y, Tajima O, et al. Regulatory mechanisms of nervous systems with glycosphingolipids. Neurochem Res. 2011;36:1578–86.
19. Hadjiconstantinou M, Neff NH. Treatment with GM1 ganglioside restores striatal dopamine in the 1-methyl-4-phenyl-1,2,3,6-tetrahydropyridine-treated mouse. J Neurochem. 1988;51:1190–6.
20. Schneider JS, Pope A, Simpson K, Taggart J, Smith MG, DiStefano L. Recovery from experimental parkinsonism in primates with GM1 ganglioside treatment. Science. 1992;256:843–6.
21. Favaron M, Manev H, Alho H, Bertolino M, Ferret B, Guidotti A, et al. Gangliosides prevent glutamate and kainate neurotoxicity in primary neuronal cultures of neonatal rat cerebellum and cortex. Proc Natl Acad Sci USA. 1988;85:7351–5.
22. Sofroniew MV, Pearson RC, Cuello AC, Tagari PC, Stephens PH. Parenterally administered GM1 ganglioside prevents retrograde degeneration of cholinergic cells of the rat basal forebrain. Brain Res. 1986;398:393–6.
23. Schneider JS, Roeltgen DP, Rothblat DS, Chapas-Crilly J, Seraydarian L, Rao J. GM1 ganglioside treatment of Parkinson's disease: an open pilot study of safety and efficacy. Neurology. 1995;45:1149–54.
24. Schneider JS, Sendek S, Daskalakis C, Cambi F. GM1 ganglioside in Parkinson's disease: Results of a five year open study. J Neurol Sci. 2010;292:45–51.
25. Schneider JS, Gollomp SM, Sendek S, Colcher A, Cambi F, Du W. A randomized, controlled, delayed start trial of GM1 ganglioside in treated Parkinson's disease patients. J Neurol Sci. 2013;324:140–8.
26. Schneider JS, Cambi F, Gollomp SM, Kuwabara H, Brašić JR, Leiby B, et al. GM1 ganglioside in Parkinson's disease: Pilot study of effects on dopamine transporter binding. J Neurol Sci. 2015;356:118–23.
27. Agnati LF, Fuxe K, Calza L, Benfenati F, Cavicchioli L, Toffano G, et al. Gangliosides increase the survival of lesioned nigral dopamine neurons and favour the recovery of dopaminergic synaptic function in striatum of rats by collateral sprouting. Acta Physiol Scand. 1983;119:347–63.
28. Hadjiconstantinou M, Mariani AP, Neff NH. GM1 ganglioside-induced recovery of nigrostriatal dopaminergic neurons after MPTP: an immunohistochemical study. Brain Res. 1989;484:297–303.
29. Skaper SD, Leon A, Toffano G. Ganglioside function in the development and repair of the nervous system. From basic science to clinical application. Mol Neurobiol. 1989;3:173–99.
30. Liu J, Wang X, Lu YQ, Duan CL, Gao G, Lu LL, et al. Pink1 interacts with alpha-synuclein and abrogates α-synuclein-induced neurotoxicity by activating autophagy. Cell Death Dis. 2017;8:e3056.
31. Su M, Shi JJ, Yang YP, Li J, Zhang YL, Chen J, et al. HDAC6 regulates aggresome-autophagy degradation pathway of α-synuclein in response to MPP+-induced stress. J Neurochem. 2011;117:112–20.
32. Chen LL, Song JX, Lu JH, Yuan ZW, Liu LF, Durairajan SSK, et al. Corynoxine, a natural autophagy enhancer, promotes the clearance of alpha-synuclein via Akt/mTOR pathway. J Neuroimmune Pharmacol. 2014;9:380–7.
33. Bhangale JO, Acharya SR. Anti-Parkinson activity of petroleum ether extract of ficus religiosa (L.) leaves. Adv Pharmacol Sci. 2016;2016:9436106.
34. Wang XH, Lu G, Hu X, Tsang KS, Kwong WH, Wu FX, et al. Quantitative assessment of gait and neurochemical correlation in a classical murine model of Parkinson's disease. BMC Neurosci. 2012;13:142.
35. Feng GS, Zhang ZJ, Bao QQ, Zhang ZJ, Zhou LB, Jiang J, et al. Protective effect of chinonin in MPTP-induced C57BL/6 mouse model of Parkinson's disease. Biol Pharm Bull. 2014;37:1301–7.
36. Vila M, Przedborski S. Targeting programmed cell death in neurodegenerative diseases. Nat Rev Neurosci. 2003;4:365–75.
37. Meredith GE, Rademacher DJ. MPTP mouse models of Parkinson's disease: an update. J Parkinsons Dis. 2011;1:19–33.
38. Kim-Han JS, Antenor-Dorsey JA, O'Malley KL. The parkinsonian mimetic, MPP+, specifically impairs mitochondrial transport in dopamine axons. J Neurosci. 2011;31:7212–21.
39. Zeng XS, Geng WS, Jia JJ. Neurotoxin-induced animal models of Parkinson disease: pathogenic mechanism and assessment. ASN Neuro. 2018;10:1759091418777438.
40. Martinez TN, Greenamyre JT. Toxin models of mitochondrial dysfunction in Parkinson's disease. Antioxid Redox Signal. 2012;16:920–34.
41. Subramaniam SR, Chesselet MF. Mitochondrial dysfunction and oxidative stress in Parkinson's disease. Prog Neurobiol. 2013;106-107:17–32.

42. Dai RW, Zhang SJ, Duan WJ, Wei RR, Chen HF, Cai WB, et al. Enhanced autophagy contributes to protective effects of GM1 ganglioside against Aβ1-42-induced neurotoxicity and cognitive deficits. Neurochem Res. 2017;42:2417–26.

43. Hwang J, Lee S, Lee JT, Kwon TK, Kim DR, Kim H, et al. Gangliosides induce autophagic cell death in astrocytes. Br J Pharmacol. 2010;159:586–603.

44. Kasahara R, Yamamoto N, Suzuki K, Sobue K. The σ1 receptor regulates accumulation of GM1 ganglioside-enriched autophagosomes in astrocytes. Neuroscience. 2017;340:176–87.

45. Kim YC, Guan KL. mTOR: a pharmacologic target for autophagy regulation. J Clin Invest. 2015;125:25–32.

46. Mizushima N, Yoshimori T, Levine B. Methods in mammalian autophagy research. Cell. 2010;140:313–26.

47. Lashuel HA, Overk CR, Oueslati A, Masliah E. The many faces of α-synuclein: from structure and toxicity to therapeutic target. Nat Rev Neurosci. 2013;14:38–48.

48. Ganley IG, Lam DH, Wang JR, Ding XJ, Chen S, Jiang XJ. ULK1.ATG13.FIP200 complex mediates mTOR signaling and is essential for autophagy. J Biol Chem. 2009;284:12297–305.

49. Mizushima N. The role of the Atg1/ULK1 complex in autophagy regulation. Curr Opin Cell Biol. 2010;22:132–9.

50. Schneider JS, Aras R, Williams CK, Koprich JB, Brotchie JM, Singh V. GM1 ganglioside modifies α-synuclein toxicity and is neuroprotective in a Rat α-synuclein model of parkinson's disease. Sci Rep. 2019;9:8362.

51. Oertel WH, Quinn NP. Parkinson's disease: drug therapy. Baillieres Clin Neurol. 1997;6:89–108.

52. Fahn S, Oakes D, Shoulson I, Kieburtz K, Rudolph A, Lang A, et al. Levodopa and the progression of Parkinson's disease. N Engl J Med. 2004;351:2498–508.

53. PD Med Collaborative Group, Gray R, Ives N, Rick C, Patel S, Gray A, et al. Long-term effectiveness of dopamine agonists and monoamine oxidase B inhibitors compared with levodopa as initial treatment for Parkinson's disease (PD MED): a large, open-label, pragmatic randomised. Lancet. 2014;384:1196–205.

54. Bibbiani F, Oh JD, Chase TN. Serotonin 5-HT1A agonist improves motor complications in rodent and primate parkinsonian models. Neurology. 2001;57:1829–34.

55. Brotchie JM. Nondopaminergic mechanisms in levodopa-induced dyskinesia. Mov Disord. 2005;20:919–31.

56. Fabbrini G, Barbanti P, Aurilia C, Pauletti C, Lenzi GL, Meco G. Donepezil in the treatment of hallucinations and delusions in Parkinson's disease. Neurol Sci. 2002;23:41–43.

57. Schapira AH, Bezard E, Brotchie J, Calon F, Collingridge GL, Ferger B, et al. Novel pharmacological targets for the treatment of Parkinson's disease. Nat Rev Drug Disco. 2006;5:845–54.

58. He Q, Koprich JB, Wang Y, Yu WB, Xiao BG, Brotchie JM, et al. Treatment with trehalose prevents behavioral and neurochemical deficits produced in an AAV α-synuclein rat model of Parkinson's disease. Mol Neurobiol. 2016;53:2258–68.

59. Sarkar S, Davies JE, Huang Z, Tunnacliffe A, Rubinsztein DC. Trehalose, a novel mTOR-independent autophagy enhancer, accelerates the clearance of mutant huntingtin and alpha-synuclein. J Biol Chem. 2007;282:5641–52.

60. Lu JH, Tan JQ, Durairajan SS, Liu LF, Zhang ZH, Ma L, et al. Isorhynchophylline, a natural alkaloid, promotes the degradation of alpha-synuclein in neuronal cells via inducing autophagy. Autophagy. 2012;8:98–108.

61. Steele JW, Ju S, Lachenmayer ML, Liken J, Stock A, Kim SH, et al. Latrepirdine stimulates autophagy and reduces accumulation of α-synuclein in cells and in mouse brain. Mol Psychiatry. 2013;18:882–8.

62. Hebron ML, Lonskaya I, Moussa CEH. Nilotinib reverses loss of dopamine neurons and improves motor behavior via autophagic degradation of α-synuclein in Parkinson's disease models. Hum Mol Genet. 2013;22:3315–28.

63. Takamura A, Higaki K, Kajimaki K, Otsuka S, Ninomiya H, Matsuda J, et al. Enhanced autophagy and mitochondrial aberrations in murine G(M1)-gangliosidosis. Biochem Biophys Res Commun. 2008;367:616–22.

64. Chan EY. Regulation and function of uncoordinated-51 like kinase proteins. Antioxid Redox Signal. 2012;17:775–5.

65. Lin MG, Hurley JH. Structure and function of the ULK1 complex in autophagy. Curr Opin Cell Biol. 2016;39:61–8.

66. Wong PM, Puente C, Ganley IG, Jiang XJ. The ULK1 complex: sensing nutrient signals for autophagy activation. Autophagy. 2013;9:124–37.